PCCP

Investigation of continuous changes of electric-field-induced electronic state in Bi1-xCaxFeO3-δ

Journal:	*Physical Chemistry Chemical Physics*
Manuscript ID:	CP-COM-05-2014-002170.R1
Article Type:	Communication
Date Submitted by the Author:	10-Jul-2014

Complete List of Authors:	Ikeda-Ohno, Atsushi; University of New South Wales, School of Civil and Environmental Engineering Lim, Ji Soo; KAIST, Department of Physics Ohkochi, Takuo; Japan Synchrotron Radiation Research Institute, Yang, Chan-Ho; KAIST, Department of Physics Seidel, Jan; University of New South Wales, School of Materials Science & Engineering

PCCP

RSCPublishing

COMMUNICATION

Investigation of continuous changes of electric-field-induced electronic state in $Bi_{1-x}Ca_xFeO_{3-\delta}$

Cite this: DOI: 10.1039/x0xx00000x

Atsushi Ikeda-Ohno,[ab] Ji Soo Lim,[c] Takuo Ohkochi,[d] Chan-Ho Yang,[ce] and Jan Seidel*[f]

Received 00th January 2012,
Accepted 00th January 2012

DOI: 10.1039/x0xx00000x

www.rsc.org/

Amongst the most interesting phenomena in correlated oxide systems are the doping-driven competitions between energetically similar ground states found in, e.g., high-Tc superconductors and colossal magnetoresistance manganites. It has recently been reported that doped multiferroics also exhibit this generic concept of phase competition. Here, we employ photoelectron emission microscopy (PEEM) to demonstrate evidence of systematic changes in the electronic structure of $Bi_{1-x}Ca_xFeO_{3-\delta}$ treated with electrically controlled hole carrier doping, the outcome of which clearly correlates to the local modulation of electronic conductivity observed in the same material.

Understanding and eventually manipulating electronic conduction in correlated oxide systems is a major goal of contemporary condensed matter physics. As a means to this end, considerable attention is focused on insulator-conductor transitions, which provide a mechanism for control of electronic states by externally applied currents or electric fields.[1] Despite this attention, many aspects of these transitions are not fully understood, particularly in multiferroic systems where the same electrons are linked to various other spin, charge and lattice degrees of freedom. In these materials, quasi-non-volatile and reversible modulation of electric conduction can be observed, e.g. through hole doping using an electric field as the control parameter.[2] The mechanism of this modulation in Ca-doped $BiFeO_3$ is based on electronic conduction as a consequence of the naturally produced oxygen vacancies that act as donor impurities to compensate calcium acceptors. Ongoing research is aimed toward a quantitative understanding of how band structure, disorder, and electron-electron interactions interact to determine the electric field and doping dependence of these effects.

The fundamental understanding of the influence of hole doping on the electronic properties of doped multiferroics, such as $Bi_{1-x}Ca_xFeO_{3-\delta}$, presents a very interesting new aspect of complex oxide functionality. Recent advances in the control of oxygen vacancies in transition metal oxides have enabled oxygen vacancy driven modifications of the magnetic, ferroelectric, and electronic properties of complex oxide materials.[3-6] Oxygen vacancies also play a critical role in the electronic properties of ferroelectric domain walls and other types of oxide interfaces that have recently received considerable interest.[7-13] Here, we explore the electronic properties of $Bi_{1-x}Ca_xFeO_{3-\delta}$ using photoemission electron microscopy (PEEM). Oxygen K edge spectra are useful to probe the local electronic properties of these materials on the micro- and nanometer scale. It is demonstrated that a high degree of control over the electronic properties of the hole doped material can be attained through local electrical switching which strongly correlates to their O K-edge XANES spectra.

$Bi_{1-x}Ca_xFeO_{3-\delta}$ is a charge-transfer-type insulator where on-site Coulomb repulsion is so strong that the lower Hubbard band of the d-orbital becomes lower than the band of the oxygen 2*p* orbital. Such an electronic structure is often found in transition metal oxide perovskites and related structures consisting of late 3*d* elements as like Fe, Co, Ni, and Cu ions which show rather strong localised character of the *d*-orbital electrons. The conduction band is mainly composed of *d* orbital states whereas valence band consists of predominantly oxygen 2*p* states.[1] Fe in this compound has a valency of 3+ and a d^5 high-spin ground state. Correspondingly, the rich fine structure of the X-ray spectra can be explained by degenerate d orbital states that are split to a t_{2g} triplet state and a e_g doublet state separated by the crystal field splitting energy ($10D_q$).

For the characterisation of local electronic structure of poled and unpoled areas, we acquired PEEM images as a function of incident X-ray energy, so-called the "image stack" method.[14] O K-edge X-ray absorption near-edge structure (XANES) spectra for different Ca-substitution levels of $Bi_{1-x}Ca_xFeO_{3-\delta}$ were extracted from these image stacks and are shown in Fig. 1. In the XANES spectra of as-grown films, we observe two lowest energy peaks located at 530 eV and 531 eV, which have information on the electronic states near the conduction band minimum. These peaks originate from the t_{2g} and e_g levels of 3*d* orbitals[15] and are detectable in the O K-edge spectra owing to *p*-*d* hybridization. When comparing measurements of the as-grown state (a) and after electrical poling (b) for samples with the same Ca-substitution level (x), the spectral features of the O K-edge are similar, except for the first peak at 528 eV (red lines in Fig. 1). This first peak at 528 eV appears after the electrical poling treatment. Its intensity increases with increasing Ca-substitution level (from x = 0.1 to 0.4).

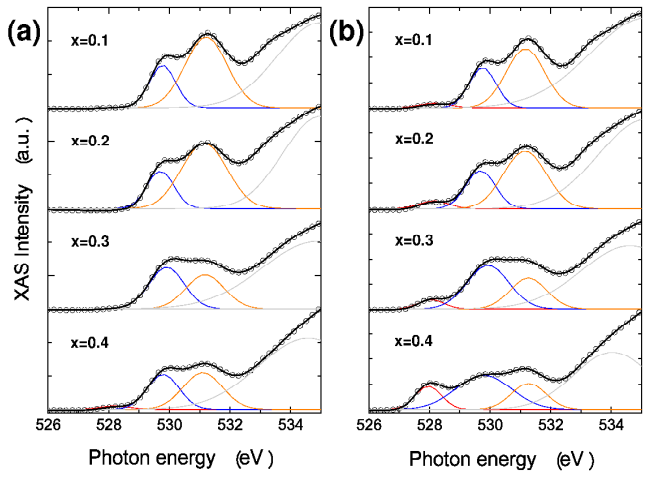

Fig. 1. O K-edge XANES spectra for different Ca-substitution ratios (x) of $Bi_{1-x}Ca_xFeO_{3-\delta}$ (circles; experimental data, lines; fitting curves): (a) as-grown state, (b) after electrical poling. Individual peak fitting is shown by coloured curves. The data have been normalized at 555 eV where the spectra don't show substitution dependent structure.[19] The spectra were produced from the intermediate point between the electrodes for each sample ("area 4" in Fig. 3).

Peak areas of the first O K-edge peaks, which are electronic bands of primarily Fe 3*d* character,[16,17] are shown as a function of Ca-substitution in Fig. 2. The intensity of Peak 2 at 530 eV (blue lines in Fig. 1) appears to be increasing with the level of Ca-substitution between x = 0.3 and 0.4, and the electrical poling process. The intensity of Peak 3 at 531 eV (orange lines in Fig. 1) shows a decreasing tendency with increasing the Ca-substitution level for the electrical poling samples (Fig. 2-(b)), whilst that for the as-grown state samples (Fig. 2-(a)) show a slight increasing tendency between x = 0.3 and 0.4. As the Ca-substitution level increases, the intensity of Peak 1 at 528 eV rises with an additional drastic increase between 30 and 40% Ca-substitution for the electrically poled samples (Fig. 2-(b)), whilst that for the as-grown state samples is almost negligible with a slight increase between 30 to 40% (Fig. 2-(a)).

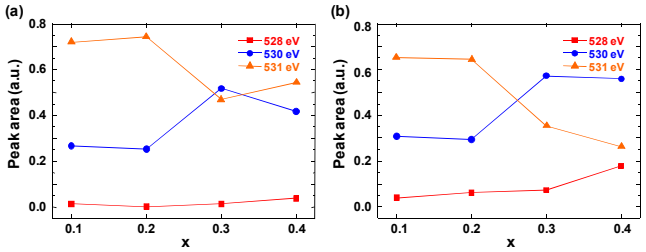

Fig. 2. Normalized peak areas of the first three O K-edge peaks as a function of Ca-substitution ratio (x): (a) as-grown state, (b) after electrical poling. The data have been normalized at 555 eV where the spectra don't show substitution dependent structure.[19]

This behaviour shows that the peak at 528 eV becomes activated upon electrical poling and is more prominent for higher Ca contents. Previous X-ray diffraction measurements have shown that an increase of Ca substitution decreases the c/a ratio.[2] With that in mind and considering Vegard's law, substitution with 40% Ca should make the material nearly cubic.[2] This in turn is expected to reduce the band gap and change the anisotropy of t_{2g} and e_g electron clouds which are coupled to this structural anisotropy.[18] The expected 3*d* level splits in octahedral (O_h) symmetry into t_{2g} and e_g levels lead to the observed relative changes in spectral weight, i.e., XANES intensity, for the peaks at 530 and 531 eV. Lowering of the peak at 531 eV and subsequent rise of the peak at 528 eV indicate a shift of spectral weight to transitions that involve the created holes in the poled state, showing that these transitions acquire a higher transition probability. Oxygen octahedral buckling in this case is reduced, reducing octahedral tilt and changing Fe–O–Fe bonding angles, which leads to changed transition probabilities due to changed orbital mixing angles. The Fe–O–Fe angle is important because it controls both the magnetic exchange and orbital overlap between Fe and O, and as such it determines the magnetic ordering temperature and the conductivity of the material.

One of the advantages of PEEM is to acquire spatially resolved XANES spectra by creating regions of interest (ROI) on the images. Fig. 3 shows the local O K-edge XANES spectra at different positions between the two electrodes used for the electrical poling treatment (gap = 20 microns, also see Electronic Supplementary Information (ESI)). When crossing the poled area (the bright coloured area in Fig. 3-(a)) between the two electrodes from left to right (i.e., from Area 1 (blue) to Area 7 (brown)), the O K-edge XANES spectra show an obvious change in the region from 527.0 to 533.0 eV (Fig. S2 in the ESI), whilst the spectral shape at the higher energy region (above 533.0 eV) is identical for different ROI areas. The spectral change observed for the lower energy peaks is depicted more clearly in Figs. 3-(c) and -(d).

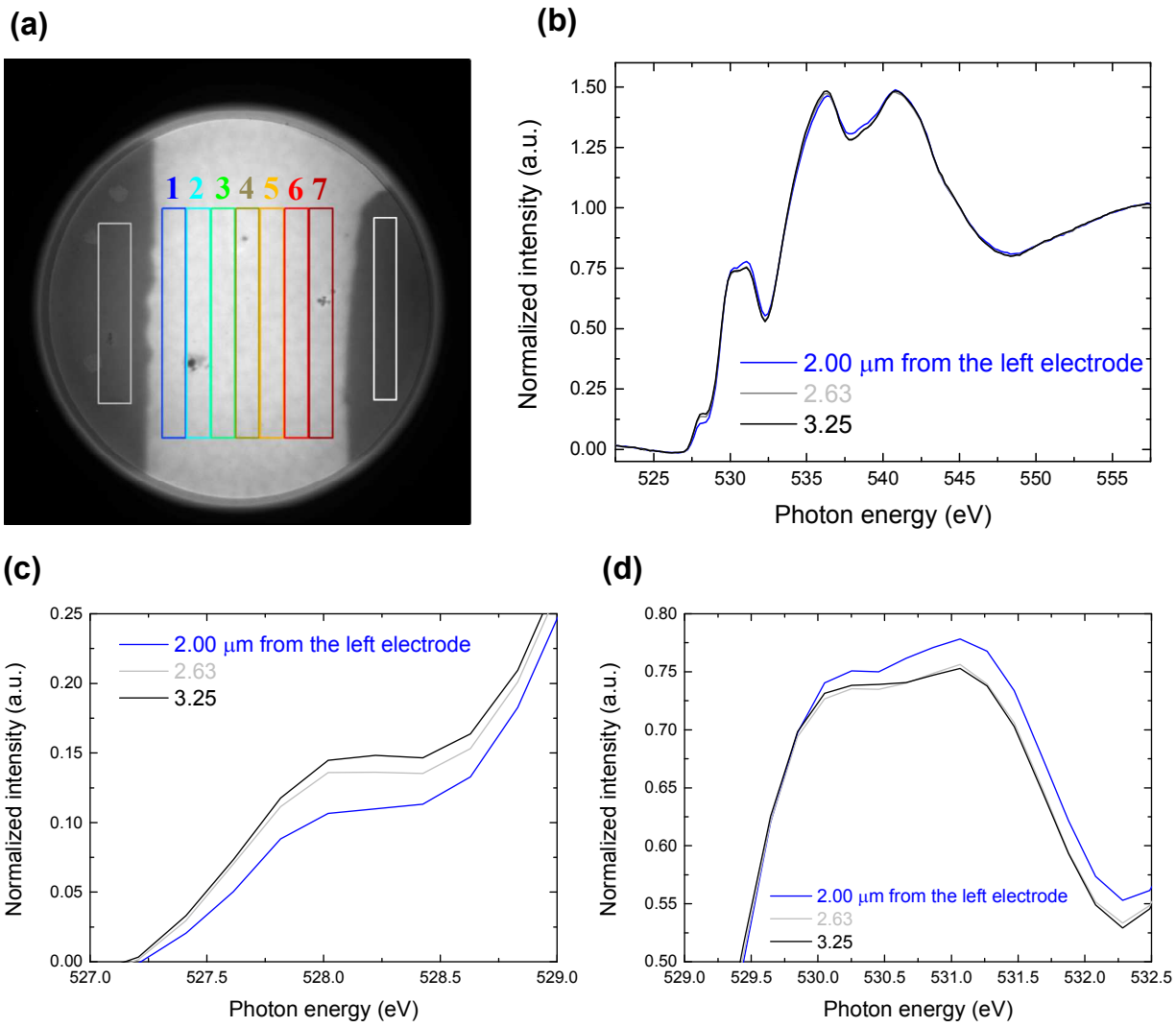

Fig. 3. (a) PEEM image of 30%-Ca substitution sample at 530.0eV. Dark areas within the circle are Pt electrodes used for electrical poling. That is, the right-side electrode was biased with a positive voltage of 15 V during the electric poling process. Electrode gap is 20 microns. Regions of interest (ROI) for acquiring local XANES spectra between the electrodes are numbered from 1 to 7 (from left to right). (b) O K-edge XANES spectra of 30%-Ca substitution sample in ROI area 1 which is the nearest to the left electrode area in (a). (c-d) Enlargement of O K-edge XANES spectra details in (b): (c) region from 527.0 to 529.0eV, (d) region from 529.0 to 532.5 eV.

Changes of peak areas for Peaks 1-3 of O K-edge XANES spectra are shown in Fig. 4. Peaks 1 and 2 at 528 and 530 eV, respectively, show a steep increase in area between ROI areas 1 and 2 (close to the left electrode), whilst their change becomes gentle from ROI areas 2 to 7. On the other hand, Peak 3 at 531 eV indicates a drastic decrease between ROI areas 1 and 2, whilst it becomes almost constant for the rest of the ROI areas. This asymmetric change can be attributed to the creation of oxygen vacancy rich and poor areas, which has also been observed over similar distances by local conductive AFM measurements of poled $Bi_{1-x}Ca_xFeO_{3-\delta}$.[2] Oxygen vacancies in this case give rise to the localisation of *d* orbitals of neighboring Fe ions, producing defect states in mid-gap. For the case of $\delta > x/2$ (n-type material),[2] which corresponds to ROI area 1, both the carrier concentration and the defect state density increase together with the oxygen vacancy density. The Fermi level lies at the defect levels partially occupying the defect states. For $\delta < x/2$ (p-type material),[2] which corresponds to ROI areas 3-7, the Fermi level is located below the valence band maximum and p-type carriers are delocalised.

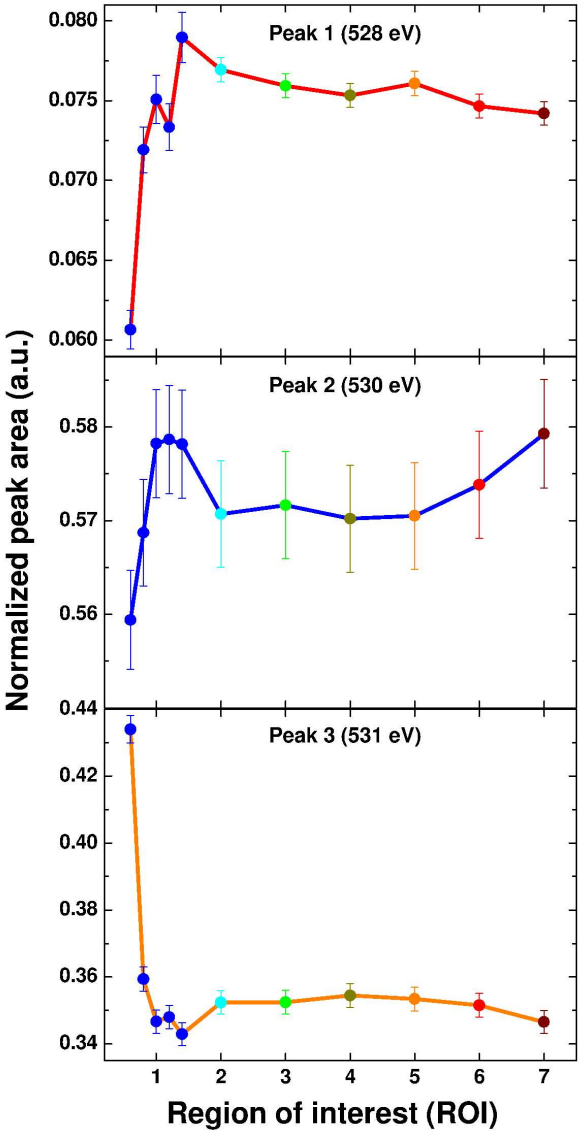

Fig. 4. Normalized peak areas of the first three O K-edge XANES peaks for Regions of Interest defined in Fig. 3-(a). The region around ROI area 1 has been further subdivided into five to show evolution of peak areas close to the electrode.

Looking at Fe $L_{II,III}$-edges XANES spectra (Fig. 5), there is no significant difference in spectral shapes between the unpoled and poled samples for the three lower Ca-substitution samples (x = 0.1 – 0.3), whilst the Fe $L_{II,III}$-edge peaks broaden towards higher energy after the poling treatment on the highest Ca-substitution sample (x = 0.4). The spectral shape for the unpoled and poled samples of x = 0.1 – 0.3 and the unpoled sample of x = 0.4 is comparable to that of Fe^{3+}perovskites,[20] whilst the observed high-energy shift/broadening on the poled samples of x = 0.4 indicates possible increase in valence states of iron, such as Fe^{4+}.[21] This indicates that the Fe oxidation state may be changed by the poling treatment particularly on the x = 0.4 sample.

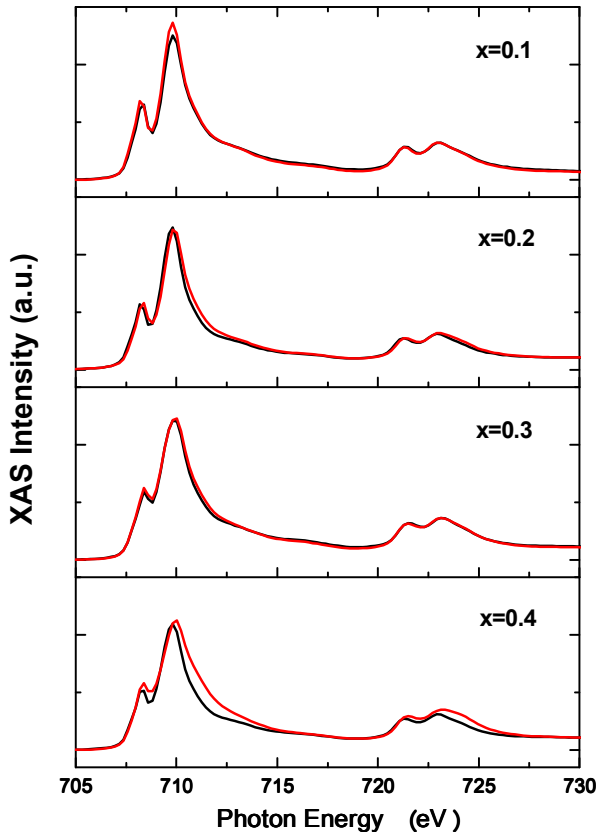

Fig. 5. Fe $L_{II,III}$-edges XANES spectra for different Ca-substitution ratios (x) of $Bi_{1-x}Ca_xFeO_{3-\delta}$. Black lines: as-grown state, red lines: after electrical poling.

In summary, based on the XAS analysis based on PEEM, we conclude that the holes created by the charge imbalance in the electrically poled $Bi_{1-x}Ca_xFeO_{3-\delta}$ give rise to an additional peak in the O K edge XANES spectra, which is substitution dependant. Conductivity of the material and amount of created holes in the poled state are correlated.[2] Our results are in qualitative agreement with other O K-edge XANES studies in hole doped correlated oxides.[22-25] The origin of the peak is yet to be understood in detail. However, it probably relates to the fact that $Bi_{1-x}Ca_xFeO_{3-\delta}$ is a charge-transfer-type Mott insulator where an extra electron is accommodated on the Fe^{3+} ion, whereas holes are located predominantly on the oxygen sites. Since $Bi_{1-x}Ca_xFeO_{3-\delta}$ has G-type antiferromagnetic order at room temperature,[26] an e_g electron with a spin at the Fe site is hybridized with 2*p* holes with the opposite spin on the surrounding oxygen ions leading to the formation of dressed hole-like particles similar to Zhang-Rice singlet states discussed in cuprates.[27-29] A detailed investigation of the possibility of a hole-like dressed particle state will be one possible future direction of our work. Many transition metal oxides, especially ferrites, have not shown a metallic state regardless of divalent ion substitutions for hole carriers. Systematic uprise of a Zhang-Rice singlet-like peak in the electrically-formed area with increasing Ca-substitution holds implications for the importance of oxygen vacancies. The observation leads us to expect that higher Ca^{2+} ion substitutions along with electrical removal of local oxygen vacancies will be most likely to yield some metallic states. It might provide a pathway to exotic electronic phenomena such as carrier-mediated

ferromagnetism, magnetoresistance and metal-insulator transitions in doped perovskite multiferroics.

Acknowledgements

We acknowledge George Sawatzky for fruitful discussions, and Masato Kotsugi and Tetsuya Nakamura for technical support on PEEM experiments. This work was supported by the National Research Foundation of Korea funded by the Korean Government (contract Nos. 2011-0016133, 2013S1A2A2035418, NRF-2013S1A2A2035418). J. S. acknowledges support by the Australian Research Council (ARC) under grant numbers FT110100523, DP140100463 and DP140102849. PEEM measurements were performed at the beamline BL25SU, SPring-8, with approval of the Japan Synchrotron Radiation Research Institute (JASRI) (Proposal No. 2013A1028). We acknowledge travel funding provided by the International Synchrotron Access Program (ISAP) managed by the Australian Synchrotron and funded by the Australian Government.

Notes and references

[a] *School of Civil and Environmental Engineering, The University of New South Wales, Sydney, NSW 2052, Australia.*
[b] *Institute for Environmental Research, Australian Nuclear Science and Technology Organisation, Locked Bag 2001, Kirrawee DC, NSW 2232, Australia.*
[c] *Department of Physics, Korea Advanced Institute of Science and Technology, Daejeon 305-701, Republic of Korea.*
[d] *Japan Synchrotron Radiation Research Institute, SPring-8, Sayo-cho, Sayo-gun, Hyogo 679-5198, Japan.*
[e] *Institute for the NanoCentury, Korea Advanced Institute of Science and Technology, Daejeon 305-701, Republic of Korea.*
[f] *School of Materials Science and Engineering, The University of New South Wales, Sydney, NSW 2052, Australia.*
E-mail: jan.seidel@unsw.edu.au

Electronic Supplementary Information (ESI) available: Detailed descriptions on sample growth, XRD measurement and electric poling process, PEEM experiment and XAS spectral acquisition from PEEM data. See DOI: 10.1039/c000000x/

1 M. Imada, A. Fujimori and Y. Tokura, *Rev. Mod. Phys.*, 1998, **70**, 1039.
2 C.-H. Yang, J. Seidel, S. Y. Kim, et al., *Nature Mater.,* 2009, **8**, 485.
3 J. F. Scott and M. Dawber, *Appl. Phys. Lett.,* 2000, **76**, 3801.
4 C. Ederer and N. A. Spaldin, *Phys. Rev. B,* 2005, **71,** 224103.
5 X. Ren, *Nature Mater.,* 2004, **3**, 91.
6 D. D. Cuong, B. Lee, K. M. Choi, H. S. Ahn, S. Han and J. Lee, *Phys. Rev. Lett.,* 2007, **98**, 115503.
7 J. Guyonnet, I. Gaponenko, S. Gariglio and P. Paruch, *Adv. Mater.,* 2011, **23**, 5377.
8 P. Mokrý, A. K. Tagantsev and J. Fousek, *Phys. Rev. B,* 2007, **75,** 094110.
9 E. A. Eliseev, A. N. Morozovska, G. S. Svechnikov, V. Gopalan and V. Y. Shur, *Phys. Rev. B,* 2011, **83**, 235313.
10 J. Seidel, *J. Phys. Chem. Lett.,* 2012, **3**, 2905.
11 J. Seidel, S.-Y.Yang, E. Alarcòn-Lladò, J. W. Ager and R. Ramesh, *Ferroelectrics,* 2012, **433**, 123.
12 J. Seidel, G. Singh-Bhalla, Q. He, et al., *Phase Transitions,* 2013, **86**, 53.
13 C.-H. Yang, D. Kan, I. Takeuchi, V. Nagarajan and J. Seidel, *Phys. Chem. Chem. Phys.,* 2012, **14**, 15953.
14 A. Scholl, J. Stöhr, J. Lüning, et al., *Science,* 2000, **287**, 1014.
15 K. T. Ko, M. H. Jung, Q. He, et al., *Nature Commun.,* 2011, **2**, 567.
16 M. Abbate, F. M. F. de Groot, J. C. Fuggle, et al., *Phys. Rev. B,* 1992, **46**, 4511.
17 F. M. F. de Groot, M. Gnom, J. C. Fuggle, et al., *Phys. Rev. B,* 1989, **40**, 5715.
18 G. Catalan and J. F. Scott, *Adv. Mater.,* 2009, **21**, 2463.
19 W. B. Wu, D. J. Huang, J. Okamoto, et al., *Phys. Rev. Lett.,* 2005, **94**, 146402.
20 J. Stöhr and H. C. Siegmann, *Magnetism*, Springer, Berlin, 2006.
21 H. J. Lee, G. Kim, J.-S. Kang, et al., *J. Appl. Phys.,* 2007, **101**, 09G523.
22 C. T. Chen, F. Sette, Y. Ma, et al., *Phys. Rev. Lett.,* 1991, **66**, 104.
23 N. Nücker, E. Pellegrin, P. Schweiss, et al., *Phys. Rev. B,* 1995, **51**, 8529.
24 P. Kuiper, G. Kruizinga, J. Ghijsen, et al., *Phys. Rev. B,* 1988, **38**, 6483.
25 A. Braun, D. Bayraktar, S. Erat, et al., *Appl. Phys. Lett.,* 2009, **94**, 202102.
26 G. Catalan, K. Sardar, N. S. Church, et al., *Phys. Rev. B,* 2009, **79**, 212415.
27 F. C. Zhang and T. M. Rice, *Phys. Rev. B,* 1988, **37**, 3759.
28 N. Plakida, *High-Temperature Cuprate Superconductors,* Springer-Verlag, Berlin, 2010.
29 D. Meyers, S. Mukherjee, J.-G. Cheng, et al., *Scientific Reports,* 2013, **3**, 1834.